An Electron Spin Resonance Study of DNA Dynamics Using the Slowly Relaxing Local Structure Model

Zhichun Liang and Jack H. Freed*

Baker Laboratory of Chemistry and Chemical Biology, Cornell University, Ithaca, New York 14853-1301

Robert S. Keyes and Albert M. Bobst

Department of Chemistry, University of Cincinnati, Cincinnati, Ohio 45221

Received: November 30, 1999; In Final Form: March 20, 2000

A systematic analysis is presented of the ESR spectra from DNA oligomers of a range of sizes, including a polymer, spin-labeled with nitroxide moieties attached by different tethers. The complexity of the DNA dynamics is dealt with by the use of the general slowly relaxing local structure (SRLS) model, wherein the nitroxide moiety is reorienting in a restricted local environment, which itself is relaxing on a longer time scale. The slower motion describes the global tumbling of the DNA lattice, and the faster motion, the internal dynamics. In the present analysis, the correlation times for the axially symmetric global tumbling were those obtained from hydrodynamic theory, while the correlation times for the internal dynamics and the order parameter, which directly measures its restricted range of motion, were determined by nonlinear least-squares fits to the spectra. The principal result is the observation and characterization of two types of spectra from these labeled DNA systems. These two spectra represent components that differ from each other with respect to their local environments, one a highly restricted site yielding a large order parameter (0.61) and slower internal motions and the other a much less restricted site (with order parameter of 0.18) and faster internal motions. Whereas the one-atom tethered DUTA exhibits both sites (in roughly 9:1 ratio with the more restricted site more prevalent), the two-atom tethered DUMTA and five-atom tethered DUAT exhibit just the more restricted site, but the five-atom tethered DUAP exhibits only the less restricted site. (DUAP differs from DUAT and the others in having a less flexible tether.) It is suggested that the spin labels trapped in the highly restricted/slow motional site have a stronger interaction with the base than those in the other site. In general, the longer the tether, the faster are the correlation times for internal dynamics. For all tethers, it is found that the correlation time for internal motion perpendicular to the internal symmetry axis systematically becomes slower as the size of the oligomer increases. It is suggested that this may be a manifestation of collective modes of motion of the DNA. It is pointed out that the simpler models used in previous ESR studies are simplified cases of the more realistic SRLS model.

1. Introduction

It has been well-known that DNA in solution is a semiflexible macromolecule which undergoes thermal fluctuations around its equilibrium conformation.[1,2] These thermal fluctuations drive various dynamical modes ranging from the internal motion within the nucleic acid to the overall tumbling of the macromolecule. The internal dynamics is of biological importance because it plays a role in expressing the genetic code and in controlling the interaction of DNA with proteins.[3] Thus a proper understanding of the biological function of DNA cannot be adequately understood without a reasonable picture of the internal dynamics.[4]

The internal dynamics in DNA has been studied extensively using a variety of spectroscopic techniques such as nuclear magnetic resonance (NMR),[5−10] electron spin resonance (ESR),[1,2,11−14] fluorescence polarization anisotropy (FPA),[15−18] and depolarized dynamic light scattering (DDLS),[4,19−21] as well as the new method of time-resolved Stokes shifts (TRSS).[22] Among these techniques, ESR is a powerful tool for elucidating the internal dynamics, due to its favorable intrinsic time scale, which is comparable to internal correlation times. At the same time, the spectral analysis becomes more complex since one needs more sophisticated dynamical models to interpret the internal dynamics.

In a spin-labeled nucleic acid, the internal dynamics usually consists of long-range collective bending and twisting modes of the bases, short-range oscillations of individual bases, and the reorientation of the spin label.[14] This greatly complicates the analysis of the ESR experiments. In previous ESR studies of DNA dynamics, controversial results have been obtained concerning the magnitude of the internal dynamics. Robinson and co-workers have employed monoacetylene- and diacetylene-tethered nitroxides to monitor the DNA dynamics.[1,3] In the theoretical model they developed, all the internal motions mentioned above are assumed to be too rapid to give rise to any residual dynamic effects. The internal dynamics is thus accounted for by its partial averaging of the electronic *g*-tensor and hyperfine tensor anisotropies. The only process in their model for which the dynamics was explicitly included is the global tumbling of the DNA duplex, which is modeled by hydrodynamic theory. The major adjustable parameter is the

* Corresponding author. E-mail: jhf@ccmr.cornell.edu. Fax: (607) 255-0595.

10.1021/jp994219f CCC: $19.00
Published on Web 05/13/2000

amplitude of the internal dynamics, which determines its partial averaging. They found that whereas, in the case of monoacetylene tether, the motion of the nitroxide is tightly coupled to that of the DNA duplex,[1] there is considerable independent motion of the probe motion for the diacetylene tether.[3] In both cases, however, only internal motions of small amplitude were detected. No rapid, large-amplitude motions of base pair were evidenced in their studies.

In contrast to the results of Robinson and co-workers, Bobst and co-workers, using a whole range of differently tethered spin labels, reported relatively large amplitude internal motions.[2,13] The nitroxide radical is attached to the base via generally more flexible tethers of different length. They analyzed their spectra in term of a base disk (BD) model, where the spin label base rather than the DNA helix is considered as the diffusing system. The spin label base is assumed to be axially symmetric, and its principal diffusion axis coincides with the bond connecting the spin label to the base. The rotation about the diffusion principal axis is found to be dependent on the tether length and is attributed to the independent motion of the nitroxide. On the other hand, the rotation perpendicular to this axis is independent of the tether length and accounts for all motions contributing to the labeled base motion including the global tumbling. They also utilized a dynamic cylinder (DC) model, which is similar to the model used by Robinson and co-workers, to interpret their ESR spectra.

It should be noted that all the theoretical models used in previous ESR spectroscopic studies of DNA dynamics are simplified ones, which effectively consider only one dynamic process. Although possibly of less biological significance compared with the internal dynamics, the global motion of the DNA helix must be explicitly accounted for, together with the internal motion, in order to provide a more complete dynamic model, with which to analyze the ESR spectra. A theoretical framework underlying such an analysis was first proposed by Freed and co-workers in another context.[23,24] They developed the slowly relaxing local structure (SRLS) model, in which the spin-bearing moiety is rotating with respect to an orienting potential, which is itself fluctuating on a slower time scale. The physics of the SRLS model resembles the dynamic picture within a DNA system, where the spin-labeled base is reorienting within the DNA body, which is itself tumbling more slowly.

The extension of the SRLS model to the ESR slow motional regime by Polimeno and Freed[25] has established a good basis for its application to DNA systems. In the latest development of the slow motional ESR theory, the SRLS model has been extended to make it suitable for the study of DNA (as well as protein) dynamics.[26] Its basic features are illustrated in Figure 1. It allows for different rotational relaxation times for the spinning motion around the long DNA helix axis ($\tau_{\parallel}^{c}$) and the motion or wobbling of this axis ($\tau_{\perp}^{c}$). In addition, it describes the internal dynamics of the nitroxide moiety by $\tau_{\parallel}^{o}$ and $\tau_{\perp}^{o}$ for motion around its principal internal axis and of the wobbling of this axis, respectively (more generally it allows for τ_{x}^{o}, τ_{y}^{o}, and τ_{z}^{o}). In addition it allows for a constraining potential for the internal motion, which directly yields the order parameters for this motion. In addition one must specify the orientation of the principal axes of internal motion related to those for the overall helix motion. The "single dynamic mode" BD and DC models are both limiting cases of the two-body SRLS model. The BD model corresponds to the limit when the internal motions are rapidly motionally narrowed (i.e. $\tau_{\perp}^{o} = \tau_{\parallel}^{o} \rightarrow 0$).[26] The DC model just assumes a simple diffusion tensor such that its $\tau_{\perp}$ reflects the overall motion and its $\tau_{\parallel}$ the internal motion

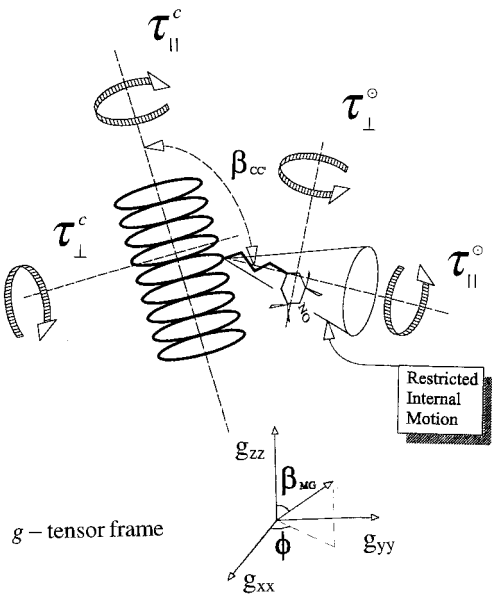

Figure 1. Slowly relaxing local structure (SRLS) model and its various model parameters applied to a DNA helix. The microscopic order but macroscopic disorder (MOMD) model is the limiting case when $\tau_{\parallel}^{c}$ and $\tau_{\perp}^{c} \rightarrow \infty$. The fast internal motion (FIM) model is another limiting case when $\tau_{\parallel}^{o}$ and $\tau_{\perp}^{o} \rightarrow 0$. The insert shows the *g*-tensor frame of the nitroxide and the orientation of the principal internal axis associated with $\tau_{\parallel}^{o}$.

(i.e. $\tau_{\parallel} = \tau_{\parallel}^{o}$ and $\tau_{\perp} = \tau_{\perp}^{c}$).[26] Liang and Freed[26] refer to the DC model as an example of the class of "fast internal motion" (FIM) models and the BD model is in the class of "very anisotropic rotational diffusion" (VAR) models. These models will be presented in more detail in section 2.

While the SRLS model offers a better approximation to the complex dynamics, its implementation requires a more powerful computational algorithm as well as richer experimental information, due to the inclusion of additional motional and structural degrees of freedom. We have developed new algorithms to address these computational difficulties.[27] In general for DNA or proteins in aqueous solution, one must determine the diffusion tensors for the overall tumbling, the diffusion tensors for the internal motion, the orientational potential (or equivalently the order parameters) restricting the internal motion, the principal axes of orientation of the internal modes relative to the principal axes of global tumbling, as well as the principal axes of the magnetic tensors relative to those of the internal motion. Clearly, to accurately determine the many dynamic and ordering parameters related to the SRLS model from the spectral analysis, extensive experimental data are highly desirable. This can, in principle, be achieved by obtaining ESR spectra on the same macromolecular system at different frequencies.[26] This approach has been demonstrated in a recent multifrequency ESR study of the protein T4 lysozyme.[28] In the fast time scale of the 250 GHz ESR experiment, the overall rotation was too slow to significantly affect the spectrum, so that it could be satisfactorily described by a microscopic order but macroscopic disorder (MOMD) model.[29] The MOMD model is a limiting case of the SRLS model in which the overall tumbling is so slow that it is effectively frozen out (i.e. $\tau_{\parallel}^{c}$ and $\tau_{\perp}^{c} \rightarrow \infty$), and only the internal dynamics is present. The fits of the MOMD model to the 250 GHz spectra thus yielded good spectral resolution for the internal dynamics. The slower time scale 9 GHz spectra, on the other hand, are sensitive to both the internal and the global dynamics. When the internal motional parameters are fixed at the values obtained from the 250 GHz data, the SRLS

fits to the 9 GHz line shapes successfully yielded the rates for the global dynamics. In this way, the two motions were separated and spectral resolution to these motions was significantly enhanced.

In the present study, we extend the ESR line shape analysis to the DNA systems extensively studied at 9 GHz by Bobst and co-workers.[2,13,14,30−32] In order to use these 9 GHz spectra, we shall adopt a different approach to deal with the global dynamics. The global tumbling rates are first estimated using hydrodynamic theory.[33] These rates are then employed in the SRLS fits to the 9 GHz spectra to extract motional and ordering parameters for the internal dynamics. We then use these parameters to compare the internal dynamics among the spin-labeled DNA systems of different tether lengths and of different oligomer sizes.

The present study represents the first application of the general (and sophisticated) SRLS model[26] (which includes anisotropic overall motion, i.e. $\tau_{\perp}^{o} \neq \tau_{\parallel}^{o}$ and arbitrary orientation of the principal axes of internal motion relative to the axes for overall motion). These features are necessary to adequately deal with the key features of spin-labeled DNA dynamics. In this work we analyze results using four differently tethered spin labels. While the results for 3 of the 4 spin labels have been presented previously[2,13,30] in the context of the simpler models, the results on the DUTA spin label (cf. below) are new and of particular importance, since they show the presence of two spectral components, as we note below.

The paper is organized as follows. In section 2, the various models used in this work and their range of validity are briefly discussed. In the following section, the results of spectral fitting are presented. For the one tether system (DUTA), reasonable fits can be obtained only when two spectral components are invoked in the SRLS analysis, as just noted. For other longer tether systems (DUMTA and DUAT), the experimental data are not of sufficient resolution to justify the presence of two components. A spectral analysis is also performed on a five tether system, DUAP, using both SRLS and simpler limiting models to test the applicability of these simpler models. In section 4, the results from section 3 are discussed in terms of the two components. The results clearly indicate the presence of a highly ordered component and a weakly ordered component, even though only one such component dominates the observed ESR spectra, with the exception of DUTA. Finally in section 4, the main conclusions are summarized.

2. Theoretical Background

2.1. Coordinate Systems. The ESR line shape is mainly determined by the intramolecular magnetic interactions of the electron spin quantized along the static magnetic field (B_0) and contained in the nitroxide moiety that is attached to the DNA helix. We therefore define two reference frames: the laboratory frame (L) with its z-axis being along the the magnetic field, B_0, and the magnetic tensor frame (G) with its z-axis being along the π orbital of the electron spin [the magnetic Zeeman (g) and hyperfine (A) frames are taken as coincident]. While L is a space-fixed frame, G is fixed in the nitroxide moiety. The transformation between the two frames is described by a set of Euler angles $\Omega_{LG} = (\alpha_{LG}, \beta_{LG}, \gamma_{LG})$ which are modulated by the various motions in the DNA system. A decomposition of Ω_{LG} may be required in order to describe the various dynamic modes of the systems under study.

Several coordinate systems are needed to describe the overall and internal motions. First is the global diffusion frame, which is fixed in the diffusing DNA and is determined by its geometry.

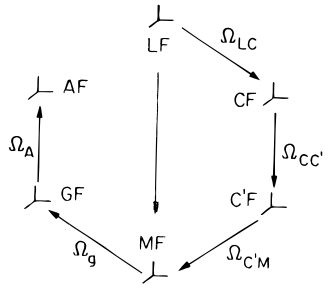

Figure 2. Reference frames which define the structural and dynamic properties of the combined system of spin-labeled moiety and DNA helix: LF = lab frame; CF = cage frame; C′F = internal director frame; MF = internal diffusion frame; GF = g tensor frame; AF = A tensor frame (from ref 26).

Since the DNA can be viewed as approximately an axially symmetric cylinder, the long axis of the DNA helix is defined as the z-axis of the global diffusion (C) frame.

For the internal motion, the spin label is the diffusing body. Since the spin label can be approximated as a rod, the z-axis of the internal diffusion frame (M) is defined to be parallel to the tether connecting the nitroxide to the base. Also, since the spin label tends to align toward the normal to the DNA helix surface, the z-axis of the internal director (C') frame is therefore taken to be approximately parallel to this normal. It should be noted that the C' frame is taken as fixed with respect to the DNA body.

The various reference frames used in this work and their relationship are given in Figure 2.

2.2. Slow-Motional ESR. The slow-motional ESR line shape based on the stochastic Liouville theory can be calculated according to[34−36]

$$I(\omega) = \pi^{-1}\langle v|[(\hat{\Gamma} - i\hat{H}^{\times}) + i\omega I]|v\rangle \qquad (1)$$

In this equation, $\hat{H}^{\times}$ is the Liouville superoperator associated with the spin Hamiltonian,

$$\hat{H} = \sum_{\mu=g,A}\sum_{l=0,2}\sum_{m=-l}^{l}\sum_{m'=-l}^{l} \hat{A}_{\mu,L}^{(l,m)}\, D_{mm'}^{l}(\Omega_{LG})\, F_{\mu,G}^{(l,m')*} \qquad (2)$$

where μ specifies the type of interactions (Zeeman or hyperfine), $F_{\mu,G}^{(l,m')}$ are components of the magnetic tensor of type μ in the G frame, $\hat{A}_{\mu,L}^{(l,m)}$ are functions of the spin operators quantized in the L frame, and the $D_{mm'}^{l}(\Omega_{LG})$ are Wigner rotation matrix elements relating the L and G frames. The time dependence of Ω_{LG} is described by the diffusion superoperator, $\hat{\Gamma}$, in eq 1, which is assumed to obey the following stochastic process:

$$\frac{\partial P(\Omega_{LG}, t)}{\partial t} = -\hat{\Gamma} P(\Omega_{LG}, t) \qquad (3)$$

Here $P(\Omega_{LG},t)$ is the probability of the spin label being in the orientation Ω_{LG} at time t. This stochastic process is also assumed to have a unique equilibrium distribution $P_0(\Omega_{LG})$, which appears in the starting vector, $|v\rangle$, in eq 1:

$$|v\rangle = (2I+1)^{-1/2}\,|S_x \otimes I_I \otimes P_0(\Omega_{LG})^{1/2}\rangle \qquad (4)$$

Here I is the nuclear spin, S_x is the x components of the electron magnetization, and I_I is a unit vector in the nuclear spin space.

2.3. SRLS Model. The detailed analytical expressions of $\hat{H}^{\times}$ and $\hat{\Gamma}$ in eq 1 have been given in previous work on the SRLS model.[25,26] To calculate the ESR line shape from eq 1,

we need to expand these superoperators in a space, which is a direct product of the various motional degrees of freedom in the system. A convenient choice of such a basis set has been introduced previously, and its angular part is given as follows:[25]

$$|L^o, M^o, K^o, L^c, M^c, K^c\rangle = \frac{\sqrt{(2L^o+1)(2L^c+1)}}{8\pi^2} \times D^{L^o}_{M^oK^o}(\Omega_{LM}) \otimes D^{L^c}_{M^cK^c}(\Omega_{LC}) \quad (5)$$

Here the Euler angles, Ω_{LM} and Ω_{LC}, describe the internal and the global motions, respectively. In this work, since both the spin label and the DNA helix are assumed to be approximately cylindrical, the diffusion tensors for these two motions are axially symmetric and each of them can be represented by two diffusion components, i.e., $\tau^o_\perp$ and $\tau^o_\parallel$ for the internal motion and $\tau^c_\perp$ and $\tau^c_\parallel$ for the overall motion (cf. Figure 1). [In refs 25 and 26, rotational diffusion tensor components $R^i_\perp$ and $R^i_\parallel$, $i =$ *o* or *c*, were used. Here we use the inverses: $\tau^i_\parallel \equiv (6R^i_\parallel)^{-1}$ and $\tau^i_\perp \equiv (6R^i_\perp)^{-1}$, $i = o$ or c, to more easily compare with the previous DNA studies].

The rotation specified by Euler angles Ω_{LG}, which appear in $\hat{H}^x$ in eq 1, can be written as the sum of two rotations, i.e., $\Omega_{LG} = \Omega_{MG} + \Omega_{LM}$, as indicated in Figure 2, where the diffusion tilt angles Ω_{MG} are time independent as discussed below. The ESR signal, which is mainly determined by $\hat{H}^x$, is therefore directly modulated only by the internal motion of the spin label. However, the spin label is rotating in an anisotropic environment due to the presence of the surrounding bases and therefore subject to an orienting potential, $U(\Omega_{C'M})$, which tends to align the spin label toward the internal director frame C'. Thus we may write

$$-U(\Omega_{C'M})/k_bT = c_0^2\, D^2_{00}(\Omega_{C'M}) + c_2^2[D^2_{02}(\Omega_{C'M}) + D^2_{0-2}(\Omega_{C'M})] \quad (6)$$

where c_0^2 and c_2^2 determine respectively the strength and the asymmetry of the potential. Again, to easily compare with the previous DNA studies, we define the order parameters S_0 and S_2,

$$S_0 = \langle D^2_{00}[\Omega_{C'M}(t)]\rangle \quad (7)$$

$$S_2 = \langle D^2_{02}[\Omega_{C'M}(t)]\rangle + \langle D^2_{0-2}[\Omega_{C'M}(t)]\rangle \quad (8)$$

which are closely related to c_0^2 and c_2^2 via the ensemble averages

$$\langle D^2_{0n}[\Omega_{C'M}(t)]\rangle = \frac{\int d\Omega\, D^2_{0n}(\Omega) \exp\left(c_0^2\, D^2_{00}(\Omega) + c_2^2[D^2_{02}(\Omega) + D^2_{0-2}(\Omega)]\right)}{\int d\Omega \exp\left(c_0^2\, D^2_{00}(\Omega) + c_2^2[D^2_{02}(\Omega) + D^2_{0-2}(\Omega)]\right)} \quad (9)$$

The Euler angles $\Omega_{C'M}$ in eq 6 can be expressed in terms of the Euler angles for the internal and global motions (cf. Figure 2): $\Omega_{C'M} = \Omega_{LM} - \Omega_{LC} - \Omega_{CC'}$. Thus, through the orienting potential, which couples the internal and global motions, the global motion is able to modulate the ESR line shape.

There are still two sets of Euler angles in Figure 2 left to be discussed. Since both the *M* and *G* frames are fixed in the spin label, the rotation specified by Euler angles Ω_{MG} is time independent and is determined by the structure of the spin label. Similarly, since both *C* and *C*′ are fixed in the DNA helix, the Euler angles $\Omega_{CC'}$ are also time independent and are determined by the structure of the DNA helix. In this work, for simplicity, it is assumed that only the polar angles, β_{MG} and $\beta_{CC'}$ need to be considered.

In summary, the SRLS model under the above simplifying approximations has four motional parameters, $\tau^o_\perp$ and $\tau^o_\parallel$ for the internal motion and $\tau^c_\perp$ and $\tau^c_\parallel$, for the overall motion, two ordering parameters, S_0 and S_2 (or alternatively c_0^2 and c_2^2), for the internal motion, and two structural parameters, β_{MG} and $\beta_{CC'}$:

$$I(\omega) = I(\tau^o_\perp, \tau^o_\parallel, t^c_\perp, \tau^c_\parallel, S_0, S_2, \beta_{MG}, \beta_{CC'}, \omega) \quad (10)$$

2.4. MOMD and FIM Models. Typically, the global tumbling of the DNA helix is about 1 order of magnitude slower than the internal dynamics of the spin label. When the global tumbling becomes sufficiently slow to be in the ESR rigid limit, the DNA helix will itself appear randomly distributed in space and static. This would be the case for a polymer of infinite length. Thus, the spin label is microscopically ordered, but the DNA helix is macroscopically disordered. The resultant MOMD model is a special case of the SRLS model in the slow global tumbling limit, as we have already noted. Mathematically, the *C* and *C*′ frames become fixed in the *L* frame and $\Omega_{LC'} = \Omega_{CC'} + \Omega_{LC}$ becomes time independent but may take all possible values over the unit sphere. Only the internal motion is observed to be time dependent and it is now described by $\Omega_{C'M}$. The line shape function for the MOMD model is a static average of individual line shape functions over $\Omega_{LC'}$ (or $\beta_{LC'}$):

$$I(\omega) = I(\tau^o_\perp, \tau^o_\parallel, S_0, S_2, \beta_{MG}, \omega) = \int \sin\beta_{LC'}\, d\beta_{LC'}\, I(\tau^o_\perp, \tau^o_\parallel, S_0, S_2, \beta_{MG}, \beta_{LC'}, \omega) \quad (11)$$

In the other limit of fast internal motion (FIM), on the ESR time scale, we cannot observe the details of the spin label internal motion but only its average orientation. This average orientation is quantified by averaging the orientation of the spin label over the internal motion, $\langle D^L_{MK}(\Omega_{C'M})\rangle$, which defines the commonly used order parameters given in eqs 7 and 8. The internal motion is therefore completely specified by the two order parameters. The ESR line shape function for the FIM model can then be expressed in the following parameter space:

$$I(\omega) = I(\tau^c_\perp, \tau^c_\parallel, S_0, S_2, \beta_{CC'}, \beta_{MG}, \omega) \quad (12)$$

3. Results

In this section, we will analyze the 9 GHz cw ESR spectra measured in Bobst's laboratory on four spin labels attached to different oligomers and polymers. The structures of the spin labels used in this work are given in Figure 3. While the spectra from the five-atom tethered (DUAT)[30,31] and two-atom tethered (DUMTA)[2] spin labels were fit to reasonable accuracy, the spectra for the one-atom tethered spin label (DUTA) cannot be reproduced with their models. The fourth spin label we will study in this work is also a five-atom tethered system (DUAP),[14] which is similar to DUAT except that it contains a five-member nitroxide ring. Our aim is to compare the different dynamic models discussed in section 2.

The magnetic *g* and *A* tensor components employed in our spectral analysis are listed in Table 1. These values had been determined by Bobst and co-workers[2,13] from simulating the rigid limit ESR spectra.

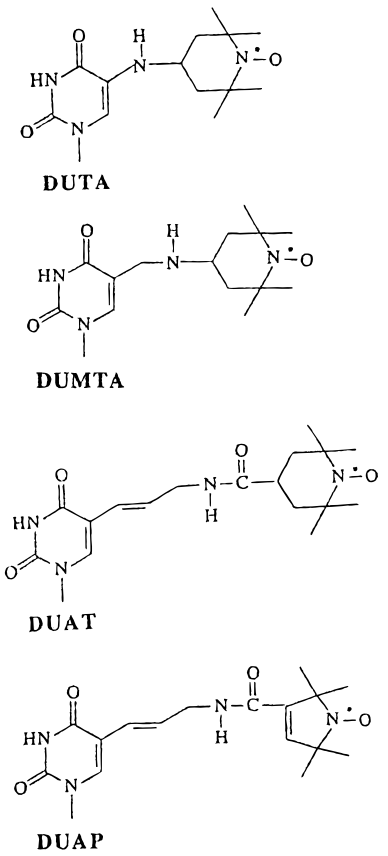

Figure 3. Structures of spin labels used in this work.

TABLE 1: Magnetic Tensor Parameters

spin label	g_{xx}	g_{yy}	g_{zz}	A_{xx} (G)	A_{yy} (G)	A_{xx} (G)
DUTA	2.0096	2.0067	2.0028	7.47	7.21	36.3
DUMTA	2.0096	2.0067	2.0028	7.47	7.21	36.3
DUAT	2.0096	2.0067	2.0028	7.47	7.49	36.9
DUAP	2.0090	2.0066	2.0029	6.25	5.70	36.0

3.1. One-Atom Tethered DUTA. DUTA is a one-atom tethered spin label which has the shortest distance between the nitroxide and the base. We present in Figure 4 the experimental spectra of four DUTA labeled molecules: 15mer, 30mer, 45mer, and polymer. The one-atom tethered DUTA was incorporated into the 15 mer $(dT)_7DUTA(dT)_7$ according to published procedures from the Bobst laboratory by using either the phosphotriester[32] or the phosphoramidite technique.[37] The DUTA-labeled 15mer was then hybridized to $(dA)_{15}$, $(dA)_{30}$, $(dA)_{45}$, and $(dA)_n$ to form the corresponding duplexes in 0.1 M NaCl/0.01 M sodium cacodylate/0.01 M $MgCl_2$, pH 7.0 buffer, and the ESR spectra were recorded as described earlier for the DUMTA-labeled system.[2]

A careful examination of these spectra shows the presence of two distinct spectral components corresponding to two distinct dynamical sites. Figure 4d for the polymer provides the clearest and most unambiguous manifestation of the second (or broader) spectral component, which is the definite extra splitting of the low-field hyperfine line (at about 3460 G) that is slightly downfield from the sharper line (at about 3468 G). This extra line is still visible but is broad in Figure 4c. In addition, in Figure 4d on the high-field side, there is a very broad feature (at about 3515 G) in addition to the main high-field hf line (at about 3502 G). Our efforts at fitting the spectra in Figure 4 with a one-component model did not succeed in fitting the extra splittings, as expected. Furthermore, the one-site model could not reproduce the line shape midway between the sharp central and high-field hf components (in the region around 3495 G) in any of the spectra of Figure 4a−d; it required the two site model to adequately fit this region, demonstrating that it is due to the central hf line of the second (i.e. the broader) component. For the existence of these two distinct spectral components, any exchange rate between them must be slower than the ESR time scale. Thus we assume that the resultant spectrum is a simple weighted sum of two individual spectra.

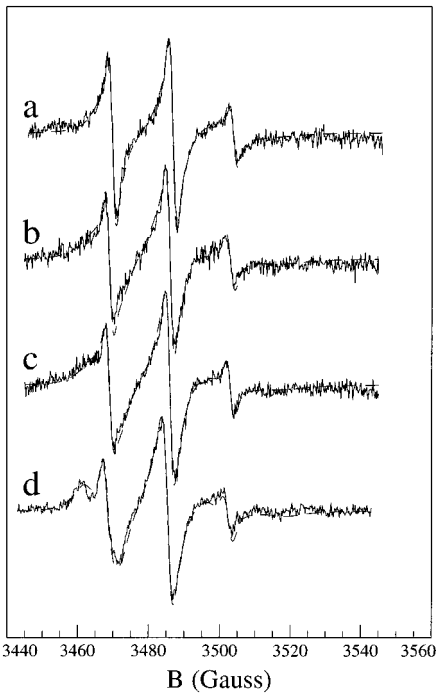

Figure 4. Nonlinear least-squares (NLLS) fits of the two-site SRLS model (dashed lines) to the experimental spectra (solid lines) of one-atom tethered DUTA spin-labeled to (a) 15mer, (b) 30mer, (c) 45mer, and (d) polymer. The best-fit parameters are presented in Table 2.

Since the polymer may be approximated as a cylinder of near infinite length, its global diffusion is considered to be in the rigid limit.[2] Therefore, the simpler MOMD model is appropriate for fitting the polymer spectrum. A preliminary fit to the polymer spectrum using the MOMD model revealed a high local ordering (with a slower dynamics) for one component and a fast local dynamics (with a lower ordering) for the other component. On the basis of this initial analysis, we could fix the potential parameter $c_0^2(2)$ at 3.0 (corresponding to $S_0 = 0.61$) and the parallel diffusion time $\tau_{||}^o(1)$ at 5.27×10^{-11} s in the fitting. The polymer spectrum was first fit by varying $\tau_{\perp}^o(1)$, $c_0^2(1)$ (or $S_0(1)$), $\beta_{MG}(1)$, $\tau_{\perp}^o(2)$, $\tau_{||}^o(2)$, $\beta_{MG}(2)$, and the Gaussian inhomogeneous broadening, ΔG. They were then used as the starting values in the spectral fittings of the other oligomers. We did not include $S_2(1)$ and $S_2(2)$ in the fits, as they would have increased the number of parameters to be fit to an unmanageable amount.

For the 45mer, 30mer, and 15mer, besides the internal motion within the DNA body, the DNA helix itself may undergo overall motion, for which the SRLS model should be suitable. The additional parameters associated with SRLS are $\tau_{\perp}^c$ and $\tau_{||}^c$ for the DNA body and $\beta_{CC'}$, the tilt angle between the ordering axis of the internal motion and the principal diffusional axis of the DNA. To reduce the number of the fitting parameters, the global diffusional rates were modeled by the hydrodynamic theory summarized by Keyes and Bobst.[2] From geometric considerations, the cage tilt was fixed at 90°. When applying the two-site model, we assumed that the two components have the same global dynamics, since each internal site is contained

TABLE 2: Two-Site SRLS Best-Fit Results for DUTA Spin-Labeled DNA[a]

	$\tau_\perp^o$ (ns)	$\tau_\parallel^o$ (ns)	β_{MG} (deg)	ΔG (G)	S_0	$\tau_\perp^c$ (ns)	$\tau_\parallel^c$ (ns)	c (%)
				15mer				
site 1	1.71	0.05	43.1	1.68	0.18	11.4	4.69	13.0
site 2	11.5	0.96	58.1	1.68	0.61	11.4	4.69	87.0
				30mer				
site 1	2.64	0.05	44.3	1.70	0.18	46.7	8.50	10.3
site 2	26.4	1.21	56.2	1.70	0.61	46.7	8.50	89.7
				45mer				
site 1	5.04	0.05	49.0	1.75	0.18	118	12.3	8.1
site 2	31.7	0.86	50.3	1.75	0.61	118	12.3	91.9
				Polymer[b]				
site 1	5.50	0.05	52.6	2.25	0.18			7.2
site 2	222	0.75	46.1	2.25	0.61			92.8
				Error (%)[c]				
site 1	20		5	3	5			
site 2	15	10	4	3				

[a] $\beta_{CC'} = 90°$ for all the SRLS fits. [b] Calculated by MOMD model, since $\tau_\perp^o$ and $\tau_\parallel^o$ are both in the rigid limit range. [c] Average error estimated from NLLS fits.[41]

within an identical DNA helix. However, each site is characterized by its own local parameters. It was assumed that the local ordering is independent of the oligomer length, which seems reasonable, and was necessary in order to reduce the parameters to be fit to a manageable number, i.e. 7. Thus, we have varied $\tau_\perp^o(1)$, $\tau_\perp^o(2)$, $\tau_\parallel^o(2)$, $\beta_{MG}(1)$, $\beta_{MG}(2)$, ΔG, and c, the percent of each component, in the SRLS fittings to the oligomer spectra. Although we let $\beta_{MG}(1)$ and $\beta_{MG}(2)$ vary, we found that the spectra showed little sensitivity to these parameters in the range 40−50°.

Figure 4 shows the best fits to the oligomer and polymer spectra by the two site SRLS and MOMD models, respectively. The best-fit parameters are given in Table 2. The spectral features characteristic of the two seemingly different states are well produced. These results indicate two spin populations, one of which shows more mobility (yielding the shaper spectrum) and one is more motionally restricted (yielding the broader spectrum). This highly ordered component has a much larger population than the other component.

3.2. DUMTA and DUAT. We next consider the two-atom and five-atom tethered spin-labels, which have a longer distance between the nitroxide and the base. We followed the same procedure as employed for the DUTA systems to analyze the DUMTA and DUTA data. However, within the spectral resolution there is no indication of the existence of two components. The spectral fits were therefore performed using one-site SRLS and MOMD models. Also preliminary fits indicated β_{MG} was about 50°, and since there was little sensitivity to changes in this value, we fixed it at 50°. Comparisons between the experimental spectra and the simulated line shapes are shown in Figures 5 and 6, and the corresponding fitting parameters are listed in Tables 3 and 4.

3.3. DUAP. Finally, we analyzed the ESR spectra of another five-atom tethered spin label, DUAP, where the nitroxide consists of a five-member ring with a double bond instead of the six-member saturated ring present in DUAT (cf. Figure 3). The spectral analysis was based on the one-site MOMD, FIM, and SRLS models with the purpose of comparing these models.

We first applied the MOMD model, which focuses on the dynamics of the local motion. In a previous study of the DUAP system, a value of 40° was obtained for the diffusion tilt angle, β_{MG},[13] and we again found little sensitivity to variation of β_{MG},

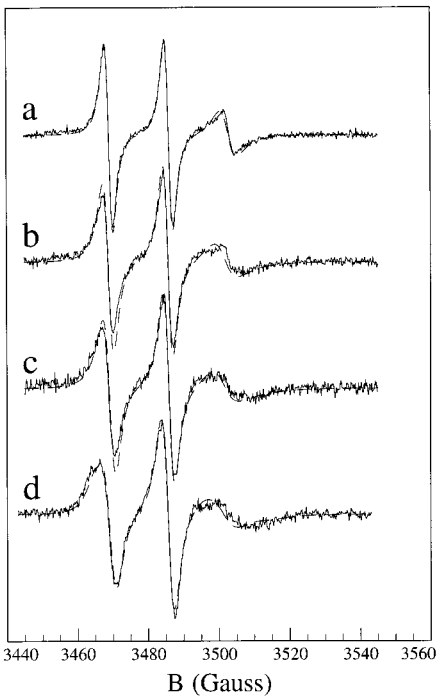

Figure 5. NLLS fits of the one-site SRLS model (dashed lines) to the experimental spectra (solid lines) of two-atom tethered DUMTA spin-labeled to (a) 15mer, (b) 30mer, (c) 45mer, and (d) polymer. The best-fit parameters are presented in Table 3.

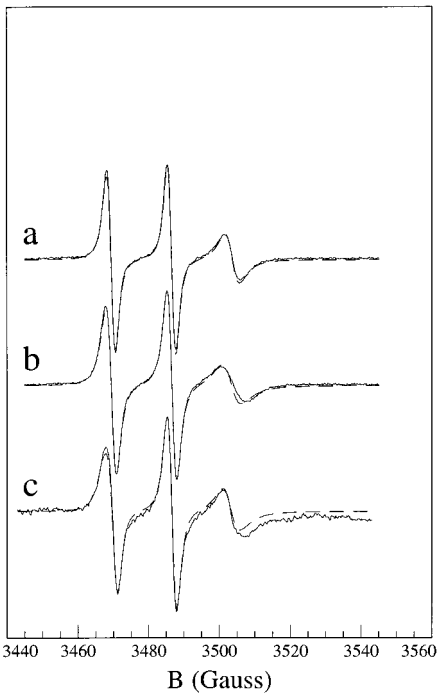

Figure 6. NLLS fits of the one-site SRLS model (dashed lines) to the experimental spectra (solid lines) of five-atom tethered DUAT spin-labeled to (a) 26mer, (b) 52mer, and (c) polymer. The best-fit parameters are presented in Table 4.

so we fixed it at 40°. The polymer spectrum was first fit by varying $\tau_\perp^o$, $\tau_\parallel^o$, c_0^2 (or S_0), and ΔG. These values were then used as the starting values in the spectral fittings of the other oligomers. However, the oligomer spectra were found to be insensitive to changes in $\tau_\parallel^o$ and it was also deemed reasonable to assume that the local ordering, S_0, is independent of the oligomer chain length. We therefore used these values for the polymer case in the oligomer spectral fits. The best fits to the

TABLE 3: One-Site SRLS Best-Fit Results for DUMTA Spin-Labeled DNA[a]

	$\tau_{\perp}^{o}$ (ns)	$\tau_{\parallel}^{o}$ (ns)	β_{MG} (deg)	ΔG (G)	S_0	$\tau_{\perp}^{c}$ (ns)	$\tau_{\parallel}^{c}$ (ns)
15mer	2.13	0.35	50	0.91	0.62	11.4	4.69
30mer	3.98	0.52	50	1.00	0.62	46.7	8.50
45mer	7.18	0.56	50	1.09	0.62	118	12.3
polymer	19.2	0.60	50	1.51	0.62		
error (%)	10	3		5	3		

[a] All footnotes given in Table 2 apply here.

TABLE 4: One-Site SRLS Best-Fit Results for DUAT Spin-Labeled DNA[a]

	$\tau_{\perp}^{o}$ (ns)	$\tau_{\parallel}^{o}$ (ns)	β_{MG} (deg)	ΔG (G)	S_0	$\tau_{\perp}^{c}$ (ns)	$\tau_{\parallel}^{o}$ (ns)
26mer	3.29	0.24	50	1.27	0.61	34.0	7.51
52mer	4.39	0.36	50	1.30	0.61	167	13.9
polymer	9.36	0.31	50	1.71	0.61		
error (%)	7	2		2	4		

[a] All footnotes given in Table 2 apply here.

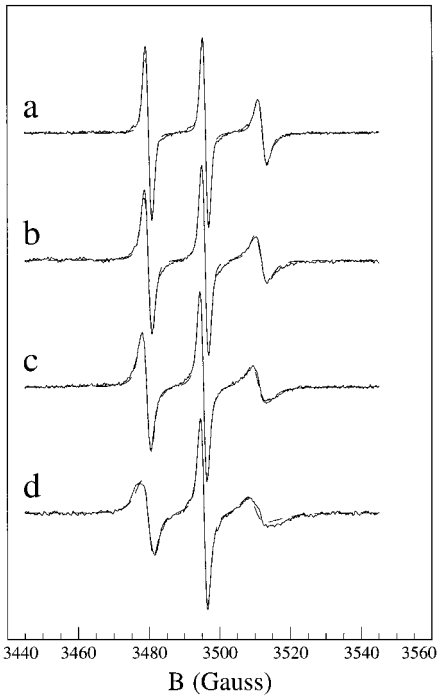

Figure 7. NLLS fits of the one-site MOMD model (dashed lines) to the experimental spectra (solid lines) of five-atom tethered DUAP spin-labeled to (a) 15mer, (b) 26mer, (c) 52mer, and (d) polymer. The best-fit parameters are presented in Table 5.

experimental spectra by the MOMD model are displayed in Figure 7, and the best fit parameters are listed in Table 5. The agreement is fairly good between the theory and experiment for all the oligomers and the polymer.

Our next attempt was to perform a similar spectral analysis based on the FIM model. In contrast to the MOMD type analysis, we started the analysis from the 15mer, since it had the fastest internal dynamics, as evidenced from the SRLS model fitting results (see below and Table 5). We first fixed the global diffusion time at the values estimated from the hydrodynamic theory. While the experimental spectrum could be reproduced by the FIM model to an acceptable accuracy for the 15mer, it was impossible to achieve overall fits for the other oligomers, due to their much slower internal dynamics (Table 5). We then allowed the global diffusion coefficients to vary in the spectral

TABLE 5: One-Site Best-Fit Results for DUAP Spin-Labeled DNA[a]

	$\tau_{\perp}^{o}$ (ns)	$\tau_{\parallel}^{o}$ (ns)	β_{MG} (deg)	ΔG (G)	S_0	$\tau_{\perp}^{c}$ (ns)	$\tau_{\parallel}^{c}$ (ns)
				SRLS			
15mer	0.87	0.14	40	1.35	0.18	11.4	4.69
26mer	2.47	0.14	40	1.23	0.18	34.0	7.51
52mer	3.66	0.14	40	1.17	0.18	167	13.9
polymer	7.31	0.14	40	1.13	0.18		
error (%)	3			2	3		
				MOMD			
15mer	0.78	0.14	40	1.38	0.18		
26mer	1.74	0.14	40	1.36	0.18		
52mer	3.19	0.14	40	1.23	0.18		
polymer	7.31	0.14	40	1.13	0.18		
error (%)	2			2	3		
				FIM			
15mer				1.39	0.58	15.6	1.49
26mer				1.31	0.58	25.8	2.58
52mer				1.23	0.58	59.1	2.15
error (%)				2	2	2	3

[a] All footnotes given in Table 2 apply here.

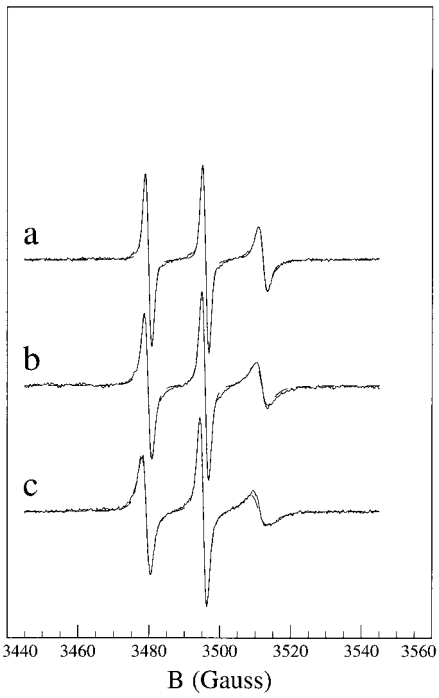

Figure 8. NLLS fits of the one-site FIM model (dashed lines) to the experimental spectra (solid lines) of five-atom tethered DUAP spin-labeled to (a) 15mer, (b) 26mer, and (c) 52mer. The best-fit parameters are presented in Table 5.

simulations, which results in improved fits to all the spectra. Finally, we let $\beta_{CC'} = 90°$, since the principal global diffusion axis and the principal internal ordering axis are perpendicular to each other. The parameters determined by the NLSL fits then included $\tau_{\perp}^{c}$, $\tau_{\parallel}^{c}$, S_0, and ΔG. The best fits of the FIM model to the experimental spectra of the DUAP in the different oligomer systems are displayed in Figure 8.

We now turn to the more complex SRLS model to analyze the DUAP data. The SRLS model explicitly includes both the internal and the global dynamics and needs a larger parameter space. In the SLRS fits, both the cage tilt, $\beta_{CC'}$, and the diffusion tilt, β_{MG}, were fixed at 90 and 40°, respectively. The fitting procedure started from the polymer data since in the slow global motional limit, the SRLS and MOMD models become identical.

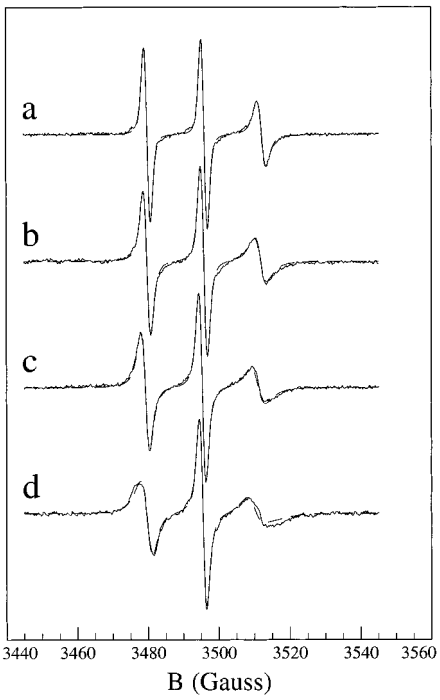

Figure 9. NLLS fits of the one-site SRLS model (dashed lines) to the experimental spectra (solid lines) of five-atom tethered DUAP spin-labeled to (a) 15mer, (b) 26mer, (c) 52mer, and (d) polymer. The best-fit parameters are presented in Table 5.

The MOMD fit to the polymer spectrum provided $\tau_{\|}^{o}$ and S_0 more accurately; thus, these values were then employed in the SRLS fits to the other oligomer spectra. Figure 9 presents the best fits of the SRLS model to the DUAP data with the corresponding fitting parameters listed in Table 5.

On the basis of a careful examination of the spectra in Figures 7−9, we find that the SRLS model is a little better in reproducing all the oligomer spectra, but rather good fits are also achieved with the simpler models. Our preferred choice of the SRLS model in this paper is based on its considerably more realistic description of the complex DNA dynamics. After all, one clearly needs to consider both the internal and overall motions. In addition, we have found that the systematic use of the SRLS model throughout this work has yielded a set of ordering and motional parameters, which are more consistent among the different oligomers and different tethers than the use of the simpler models. The fact that the simple MOMD and FIM models can provide adequate fits is a consequence of the limited resolution provided by the 9 GHz ESR spectra, as discussed at considerable length elsewhere.[26] The question we now wish to address is the applicability and limitations of the simpler MOMD and FIM models when compared to the more complete SRLS model.

We do find that the MOMD values for $\tau_{\|}^{o}$ (as well as ΔG) roughly approximate those from the SRLS fit but are consistently a little faster (i.e. smaller). This is reasonable, because in the MOMD approximation the overall tumbling is neglected, so the internal motional fitting parameters must be made somewhat faster to compensate. When we compare the FIM parameters to those from the SRLS model we find that the $\tau_{\perp}^{c}$ and $\tau_{\|}^{c}$ estimated by FIM are mostly faster (and inconsistent with hydrodynamic theory), and the S_0 is considerably greater. This is because the FIM model fails to include the finite (as opposed to infinitely fast) rates of the internal motional modes, and it compensates by restricting the range of motion with the larger S_0 and a readjustment of the overall motional correlation times. In fact, the internal motional correlation times (especially $\tau_{\perp}^{o}$) are much too slow to justify the FIM model at all. Thus we conclude that the FIM model may not be as successful an approximate model for those DNA systems. Although the MOMD model also predicts a faster internal motion, it is a better representative of the SRLS model for the DNA systems under study, because of the slowness of the overall motion, and it is recommended when only limited experimental data and/or computational power are available.

4. Discussion

The most striking result of this work is the finding of two spectral components from the DNA systems. This is most clearly evidenced in the DUTA spectra (Figure 4), which cannot be satisfactorily fit with a one-site model. The two components are found to differ from each other in their local dynamics such that the spin label experiences two local environments: a highly ordered/slow dynamical site and a weakly ordered/fast dynamical site. From Table 2 it is clear that the spin label is predominantly in the highly ordered site.

Such a two-component feature appears to be in another DNA system previously studied by Robinson and co-workers.[3] Their experimental spectrum of a two-atom monoacetylenic tethered spin label (referred to as T*) shown in Figure 6 of ref 3 appears to be a superposition of individual spectra corresponding to two components of different local ordering/dynamics. A one-site model was used by these workers to fit the spectrum, and the internal motion was found to be of small amplitude. In the light of our results with DUTA, we suspect that, besides the highly ordered component, there is a low-ordering component, which was not considered in their spectral fit.

In our previous multifrequency ESR study of T4 lysozyme,[28] two distinct motional/ordering modes of the probe were also found. A possible explanation for the two modes in the T4 lysozyme study is that the nitroxide side-chain mobility on the exposed surfaces of α-helices is mainly determined by the interaction of the disulfide with the protein backbone.[38,39] For solvent-exposed helical surface sites, a possible mechanism for this interaction may be due to the adsorption of the disulfide to the helix backbone. The results therefore indicate that some of the disulfide groups are adsorbed onto the helix surface by van der Waals interactions. This results in a slower disulfide rotation constrained to a smaller space, in comparison with those disulfide groups which are not involved in van der Waals contact with the backbone.

A similar explanation may also apply to the DUTA system. Molecular modeling studies[31] suggest that the DUTA is close enough to the sugar phosphate backbone (cf. Figure 10A) to give rise to two distinct energy minima (sites). The nitroxide trapped in the highly ordered/slow motional site experiences additional interactions with the sugar phosphate backbone. Note that Keyes and Bobst in ref 14 show spectra from the zero-tethered label DUNtB that also reveal the presence of more than one component, but no quantitative interpretation has yet been attempted. For the longer (five-atom) tethered DUAP (cf. Figure 10C where the label is the five-atom tethered DUAT), the nitroxide is not only further removed from the helical DNA axis but in addition the five-membered nitroxide contains a double bond (cf. Figure 3) allowing a more rigid coupling of the ring to the amide linkage. This reduction in flexibility may be the reason why the nitroxide in DUAP is less likely to find itself in a trapped site near the sugar phosphate backbone and resides preferentially in the most extended conformation. The spectra suggest the presence of only one component with DUAP,

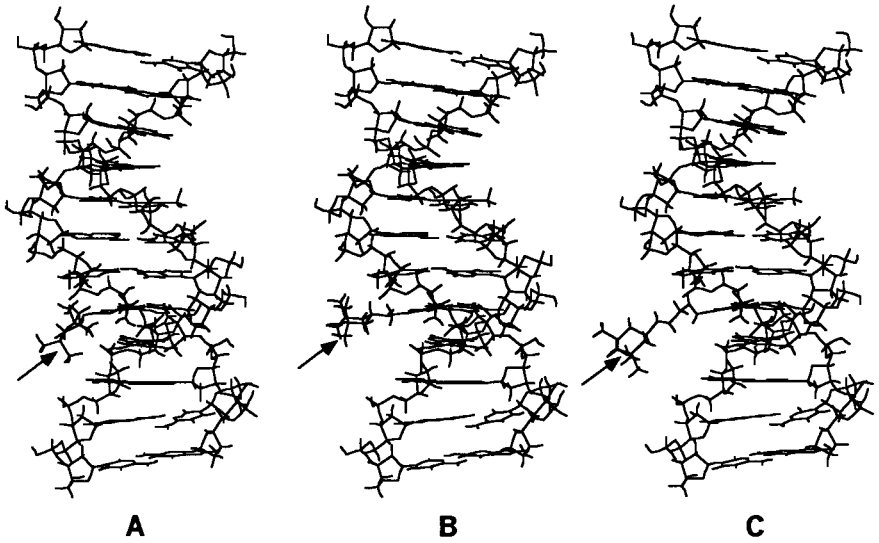

Figure 10. Molecular models of (A) DUTA-labeled, (B) DUMTA-labeled, and (C) DUAT-labeled dodecamers. Arrows point toward the nitroxide ring. The nitroxide labels were constructed with the Builder module of Insight II (MSI), and the resulting structures were put through a steepest descents minimization. All labels are shown in the most extended conformation.

although a careful inspection of its polymer spectra (cf. Figures 7 and 9) reveals a very small population of a highly ordered/slow-motional component.

The observation of the existence of two sites of different dynamics is further evidenced by the experimental spectra of the two-atom tethered DUMTA (cf. Figure 5). From Figure 10B, it is evident that the nitroxide ring is close enough to the sugar phosphate backbone to be trapped in a highly ordered/slow-motional site. The two-site feature is by far less pronounced than in the DUTA or DUNtB system but is more noticeable than in the DUAT and DUAP systems. There is a hint of a splitting in both the low-field and high-field lines, especially in the case of the polymer spectra.

To study the tether length dependence of the internal ordering and dynamics for the weakly ordered component, we first compare the best-fit parameters summarized in Table 2 for site 1 of the DUTA systems with those obtained for the DUAP system with the SRLS model (cf. Table 5). The ordering of the five-atom tethered five-membered ring nitroxide (DUAP) is virtually the same as that for the weakly ordered component of the one-atom tethered DUTA. Since the internal ordering is low, the nitroxide experiences more independent motions, which is likely to be the case if its site is located close to the center of the major groove, as shown for example for the nitroxide of DUAT in Figure 10C. It should be noted that the nature of the two tethers differs in respects other than their lengths. While DUTA has a one-atom tether with a saturated six-membered nitroxide, DUAP contains an unsaturated five-membered nitroxide, which with its double bond is more rigidly coupled to the amide linkage of the tether. This appears to show up in the slower $\tau_{\|}^{o}$ of DUAP than DUTA, i.e. in the motion around the tether "axis". The more rigid coupling of the nitroxide ring to the amide bond in DUAP may be the reason why this label does not yield the highly ordered site presumably arising from a trapped state (cf. above). There is a significant dependence of $\tau_{\perp}^{o}$ on oligomer size, indicating that $\tau_{\perp}^{o}$ is monitoring the base dynamics, as we discuss below.

It is also of interest to compare the results in Table 2 for the highly ordered component (site 2) of DUTA with those in Tables 3 and 4 for DUMTA and DUAT, respectively, which correspond to high ordering. The dominance of a highly ordered/slow-motional site in the case of the five-atom tethered DUAT comes as a surprise and is believed to arise from the flexible six-membered nitroxide ring in DUAT that allows close contact with the sugar phosphate backbone. While the local ordering (S_0) is found to be independent of the tether length, the internal dynamics characterized by both $\tau_{\|}^{o}$ and $\tau_{\perp}^{o}$ shows a general trend of being faster the longer the tether length. The nitroxides residing in the highly ordered state are more strongly coupled to the DNA helix and are expected to more closely reflect the internal nucleic acid dynamics. Thus, it may be expected that the internal motion of the highly ordered site would be independent of the tether length. This inconsistency may be due to several factors: (1) The longer chain tethers still allow for substantial internal motional rates even though these motions are constrained. (2) Since the DUMTA and DUAT spectra have been fitted using the one-site SRLS model, the $\tau_{\|}^{o}$ and $\tau_{\perp}^{o}$ listed in Tables 3 and 4 could involve some degree of averaging of some highly ordered component with dominant weakly ordered coomponent such that as the tether length gets longer, the population of the weakly ordered component becomes larger (cf. Table 2), which leads to a faster average local dynamics. At present, we have no evidence for factor 2 and we believe that factor 1 is the case. After all, motional rate constants are dynamic parameters while ordering potentials are static or equilibrium properties.[36] Thus, while the nitroxide moiety experiences the same equilibrium orientational potential well, the increased flexibility of the chain can produce faster motional rate constants.

We now wish to discuss the general observation, true for all the tethers, that the internal motions yielding $\tau_{\perp}^{o}$ becomes slower systematically as the size of the oligomer increases. [Recall that in several cases $\tau_{\|}^{o}$ was not very sensitive to the fits, so it was kept constant vs oligomer size; in other cases where $\tau_{\|}^{o}$ was allowed to vary with oligomer size, its value did remain essentially constant (cf. Tables 2−5).] One might try to attribute this to a defect in the hydrodynamic formulas[33] used to predict $\tau_{\perp}^{c}$ and $\tau_{\|}^{c}$ which then would corrupt our results for $\tau_{\perp}^{o}$. Aside from the fact that previous studies have justified their reliability,[40] our analysis in Table 5 for DUAP, which is a case of weak ordering, has shown that even by ignoring the overall tumbling by using the MOMD model, the changes in $\tau_{\perp}^{o}$ from using the MOMD model instead of SRLS was small

as compared to the variation of $\tau_{\perp}^{o}$ with oligomer size. This is because the $\tau_{\perp}^{c}$ and $\tau_{\parallel}^{c}$ are systematically longer than the $\tau_{\perp}^{o}$ (and $\tau_{\parallel}^{o}$), so their effect on the spectrum, while significant, is not as large as the latter. We therefore suggest that this increase in $\tau_{\perp}^{o}$ with oligomer size may be a manifestation of the collective bending and twisting modes (cf. Figure 2 of ref 26) of the DNA, which does depend on the oligomer size, such that their correlation times increase with increasing oligomer length.[1] This is a matter for further study.

Finally, we briefly comment on the past controversial results concerning the magnitude of the internal dynamics. In this work, we have found that there are usually two environments of different ordering/dynamics for the spin label in a DNA system. Robinson and co-workers appear to have monitored the highly ordered/slow motional site, whereas Bobst and co-workers concentrated on the weakly ordered/fast motional site, since both research groups used one-site models to fit their experimental data. While the two-site feature is clear from the spectra of the one-atom tethered spin label, DUTA, it is not so apparent with the longer-tethered spin labels except in the presence of polymer matrices (which incidentally are the biologically meaningful systems to study). Future multifrequency ESR[26,28] studies should enable further insights into the complex dynamics of spin-labeled DNA.

Acknowledgment. We wish to acknowledge helpful discussions with Dr. Jeff Barnes. This work was supported by Grants from the NIH and NSF. The computations were performed at the Cornell Theory Center.

References and Notes

(1) Hustedt, E. J.; Spaltenstein, A.; Kirchner, J. J.; Hopkins, P. B.; Robinson, B. H. *Biochemistry* **1993**, *32*, 1774.
(2) Keyes, R. S.; Bobst, A. M. *Biochemistry* **1995**, *34*, 9265.
(3) Hustedt, E. J.; Kirchner, J. J.; Spaltenstein, A.; Hopkins, P. B.; Robinson, B. H. *Biochemistry* **1995**, *34*, 4369.
(4) Patkowski, A.; Eimer, W.; Dorfmüller, Th. *Biopolymers* **1990**, *30*, 975.
(5) Lipari, G.; Szabo, A. *Biochemistry* **1981**, *20*, 6250.
(6) Lipari, G.; Szabo, A. *J. Am. Chem. Soc.* **1982**, *104*, 4546.
(7) Lipari, G.; Szabo, A. *J. Am. Chem. Soc.* **1982**, *104*, 4559.
(8) Alam, T. M.; Drobny, G. P. *Chem. Rev.* **1991**, *91*, 1545.
(9) Borer, P. N.; LaPalnte, S. R.; Kumar, A.; Zanatta, N.; Martin, A.; Hakkinen, A.; Levy, G. C. *Biochemistry* **1994**, *33*, 2441.
(10) Gaudin, F.; Chanteloup, L.; Thuong, N. T.; Lancelot, G. *Magn. Reson. Chem*. **1997**, *35*, 561.
(11) Robinson, B. H.; Drobny, G. *Annu. Rev. Biophys. Biomol. Struct*. **1995**, *24*, 523.
(12) Robinson, B. H.; Mailer, C.; Drobny, G. *Annu. Rev. Biophys. Biomol. Struct*. **1997**, *26*, 629.
(13) Keyes, R. S.; Bobst, E. V.; Cao, Y. Y.; Bobst, A. M. *Biophys. J*. **1997**, *72*, 282.
(14) Keyes, R. S.; Bobst, A. M. In *Biological Magnetic Resonance, Volume 14: The Next Millennium*; Berliner, L., Ed.; Plenum Press: New York, 1998; Chapter 7.
(15) Schurr, J. M.; Fujimoto, B. S.; Wu, P.; Song, L. In *Topics in Fluorescence Spectroscopy, Volume 3: Biological Applications*; Lakowicz, J. R., Ed.; Plenum Press: New York, 1992.
(16) Nuutero, S.; Fujimoto, B. S.; Flynn, P. F.; Reid, B. R.; Ribeiro, N. S.; Schurr, J. M. *Biochemistry* **1994**, *34*, 463.
(17) Schurr, J. M.; Fujimoto, B. S. *Biopolymers* **1999**, *49*, 355.
(18) Barone, F.; Matzeu, M.; Mazzei, F.; Pedone, F. *Biophys. Chem*. **1999**, *78*, 259.
(19) Sortie, S. S.; Pecora, R. *Macromolecules* **1988**, *21*, 1437.
(20) Patkowski, A.; Eimer, W.; Dorfmüller, Th. *Biopolymers* **1990**, *30*, 93.
(21) Eimer, W.; Williamson, J. R.; Boxer, S. C.; Pecora, R. *Biochemistry* **1990**, *29*, 799.
(22) Brauns, E. B.; Madaras, M. L.; Coleman, R. S.; Murphy, C. J.; Berg, M. A. *J. Am. Chem. Soc*. **1999**, *121*, 11644.
(23) Polnaszek, C. F.; Freed, J. H. *J. Phys. Chem*. **1975**, *79*, 2283.
(24) Freed, J. H. *J. Chem. Phys*. **1977**, *66*, 4183.
(25) Polimeno, A.; Freed, J. H. *J. Phys. Chem*. **1995**, *99*, 10995.
(26) Liang, Z.; Freed, J. H. *J. Phys. Chem*. **1999**, *103*, 6384.
(27) Liang, Z.; Freed, J. H. Manuscript in preparation, 1999.
(28) Barnes, J. P.; Liang, Z.; Mchaourab, H. S.; Freed, J. H.; Hubbell, W. L. *Biophys. J*. **1999**, *76*, 3298.
(29) Meirovitch, E.; Nayeem, A.; Freed, J. H. *J. Phys. Chem*. **1984**, *88*, 3454.
(30) Bobst, A. M.; Pauly, G. T.; Keyes, R. S.; Bobst, E. V. *FEBS Lett*. **1988**, *228*, 33.
(31) Keyes, R. S. Probing Nucleic Acid Dynamics and Protein-Nucleic Acid Interaction. Ph.D. Dissertation, University of Cincinnati, 1994.
(32) Duh, J.-H.; Bobst, A. M. *Helv. Chim. Acta* **1991**, *74*, 739.
(33) Tirado, M. M.; Torre, J. G. de la *J. Chem. Phys*. **1980**, *73*, 1986.
(34) Freed, J. H. In *Spin Labeling: Theory and Applications*; Berliner, L., Ed.; Academic Press: New York, 1976; p 53.
(35) Schneider, D. J.; Freed, J. H. *Adv. Chem. Phys*. **1989**, *73*, 387.
(36) Schneider, D. J.; Freed, J. H. In *Biological Magnetic Resonance*, Berliner, L. J., Reuben, J., Eds.; Plenum Publishing Corp.: New York, 1989; Vol. 8.
(37) Persichetti, R. A.; Sinden, R. R.; Duh, J.-L.; Bobst, A. M. *Synth. Commun*. **1991**, *21*, 1013.
(38) Mcharourab, H. S.; Lietzow, M. A.; Hideg, K.; Hubbell, W. L. *Biochemistry* **1996**, *35*, 7692.
(39) Mchaourab, H. S.; Oh, K. J.; Fang, C. J.; Hubbell, W. L. *Biochemistry* **1997**, *36*, 307.
(40) Schurr, J. M.; Schmitz, K. S. *Annu. Rev. Phys. Chem*. **1986**, *37*, 271.
(41) Budil, D. B.; Lee, S.; Saxena, S.; Freed, J. H. *J. Magn. Reson*. **1996**, *120*, 155.